

# A thermoeconomic model of a photovoltaic heat pump

R. Mastrullo<sup>b</sup>, C. Renno<sup>a,\*</sup>

<sup>a</sup> Department of Mechanical Engineering, University of Salerno, Via Ponte Don Melillo, 84084 Fisciano (Salerno), Italy

<sup>b</sup> DETEC, University of Napoli Federico II, P.le Tecchio 80, 80125 Napoli, Italy

## ARTICLE INFO

### Article history:

Received 1 August 2009

Accepted 20 April 2010

Available online 28 April 2010

### Keywords:

Photovoltaic evaporator

Heat pump

Modelling

Thermoeconomic analysis

## ABSTRACT

In this paper the model of a heat pump whose evaporator operates as a photovoltaic collector, is studied. The energy balance equations have been used for some heat pump components, and for each layer of the photovoltaic evaporator: covering glaze, photovoltaic modules, thermal absorber plate, refrigerant tube and insulator. The model has been solved by means of a program using proper simplifications. The system input is represented by the solar radiation intensity and the environment temperature, that influence the output electric power of the photovoltaic modules and the evaporation power. The model results have been obtained referring to the photovoltaic evaporator and the plant operating as heat pump, in terms of the photovoltaic evaporator layers temperatures, the refrigerant fluid properties values in the cycle fundamental points, the thermal and mechanical powers, the efficiencies that characterize the plant performances from the energy, exergy and economic point of view. This study allows to realize a thermoeconomic comparison between a photovoltaic heat pump and a traditional heat pump under the same working conditions.

© 2010 Elsevier Ltd. All rights reserved.

## 1. Introduction

The direct use of solar energy as primary energy source is interesting because of its universal availability and low environmental impact. Solar heating applications are intuitive; on the contrary, the solar energy use to obtain refrigeration is less intuitive. Different technologies can be adopted to get refrigeration from solar energy: thermal and electric solar systems, and some new emerging technologies [1]. The solar thermal systems include absorption [2], adsorption [3], solar ejector [4], thermo-mechanical and regenerative desiccant solutions [5]. As for the solar electric systems, the photovoltaic solar is the most popular technology. In fact referring to a traditional vapour plant, the compressor motor can be electrically supplied by photovoltaic modules that allow the direct conversion of solar radiation into direct current [6]. The PV system is most appropriate for small capacity refrigeration plants used for food or medical applications in areas far from conventional energy sources [7], where a high level of solar radiation is present. Moreover, the solar assisted heat pump (SAHP), introduced by [8], allows improvements in comparison with a traditional heat pump [9]; in [10,11] some experimental and theoretical studies of a SAHP are presented. Lately the solar energy conversion into electricity, by means of photovoltaic modules placed on the house roof, is widely used, but the PV module electric efficiency is about 15% and the

greater part of solar radiation is converted into heat. Hence, the hybrid photovoltaic/thermal systems (PV/T) have been designed to recover contemporaneously electrical and thermal energy. Several experimental and theoretical studies have been realized on the PV/T systems [8,12,13]. Moreover, the photovoltaic heat pump is also a promising technology, where the photovoltaic collector is used as evaporator [14]; it is possible to use the evaporator refrigeration effect to cool the solar cells with a photovoltaic efficiency increase. The solar radiation is partially transformed into electric energy by photovoltaic modules, while most of it is absorbed from the refrigerant fluid whose values of pressure and temperature rise during the day with a heat pump performances improvement. In cold winter the PV collector protects the evaporator from frosting. This paper aims at studying the dynamic model of a heat pump whose evaporator works as a PV collector. The model results have been obtained referring to the PV evaporator and the plant operating as heat pump, in terms of evaporator temperatures, refrigerant fluid properties in the cycle fundamental points, thermal and mechanical powers and efficiencies that characterize the plant performances. This analysis allows to compare from the thermoeconomic point of view a PV heat pump with a traditional plant under the same operating conditions.

## 2. Description of the photovoltaic heat pump

In the model analysed, the plant works as photovoltaic heat pump (Fig. 1) and is mainly made up of a variable speed

\* Corresponding author. Tel.: +39 089 964327; fax: +39 089 964037.  
E-mail address: [crenno@unisa.it](mailto:crenno@unisa.it) (C. Renno).

Nomenclature		Greek symbols	
$A$	heat exchange surface area ( $m^2$ )	$\alpha$	absorption coefficient
$C$	cost (€)	$\beta_{cf}$	covering factor of the solar cells
$c$	specific cost (€); specific heat ( $J/kg\ K$ )	$\delta$	efficiency defect
COP	coefficient of performance	$\varepsilon$	emissivity
$D$	diameter (m)	$\eta$	efficiency
DPB	discount pay-back (year)	$\theta_1$	incidence angle of the sunbeam
EVA	ethylene-vinyl-acetate	$\theta_2$	refracting angle of the sunbeam
$\dot{G}$	solar radiation flux (W)	$\nu$	amortization coefficient (1/year)
$h$	heat transfer coefficient ( $W/m^2K$ ); enthalpy ( $kJ/kg$ )	$\rho$	density ( $kg/m^3$ )
$H_{va}$	expansion valve coefficient	$\sigma$	Stefan-Boltzmann constant ( $W/m^2\ K^4$ )
$I$	solar radiation intensity ( $W/m^2$ )	$\tau$	transmittance coefficient
$k$	thermal conductivity ( $W/m\ K$ )	<i>Subscripts</i>	
$\dot{L}$	Power (W)	a	air; air gap
$\dot{m}$	refrigerant mass flow rate ( $kg/s$ )	b	absorber
$m$	mass (kg)	c	collector
NPV	net present value (€)	co	condensation; condenser
$n$	rotational speed (rps)	cp	compressor
$p$	pressure (bar)	e	electric energy
PV	photovoltaic	ev	evaporation; evaporator
$\dot{Q}$	thermal power (W)	ex	exergetic
$R$	refractive index	g	glazing
SPB	simple pay-back (year)	i	insulator; initial
$s$	thickness (m)	in	inlet
$T$	temperature ( $^{\circ}C$ )	k	component
$t$	time (s)	o	outdoor
$T_1$	evaporator outlet temperature ( $^{\circ}C$ )	out	outlet
$T_2$	compressor outlet temperature ( $^{\circ}C$ )	p	photovoltaic plate; peak
$T_3$	condenser outlet temperature ( $^{\circ}C$ )	pv	photovoltaic
$T_4$	evaporator inlet temperature ( $^{\circ}C$ )	r	refrigerant
TPT	tedlar-polyester-tedlar	s	sky
$V$	piston displacement volume ( $m^3$ )	t	tube; thermal
$v_1$	compressor inlet specific volume ( $m^3/kg$ )	tc	condenser tube
$x$	optimization variable	tot	total
$z$	pitch (m)	v	volumetric
		va	valve
		w	water
		hp	heat pump

compressor, an electronic expansion valve, a plate-type water condenser, a PV evaporator that works in parallel with an air evaporator; the refrigerant fluid is R22. The main component is the PV evaporator that consists of: covering glaze, photovoltaic modules, thermal absorber plate, refrigerant tubes and insulator. The removable *covering glaze* allows both to decrease the outward thermal dispersions of the collector superior surface and to assure mechanical protection; besides, it operates also as concentrating lens. An air gap allows a good thermal insulation and, instead of air, other insulators could be used. The *photovoltaic modules* are placed on the absorber plate superior surface, connected by means of gluing with high conductivity resins. The materials used for the photovoltaic cells are mainly the single-crystal silicon, the polycrystalline silicon or the amorphous silicon that differ both in terms of electric performances and manufacture costs. A limited energy conversion is possible; in fact only 5–15% of the solar radiation incident on the collector is transformed into electric energy according to the material and temperature of the panels and the solar radiation incidence angle. To obtain a high thermal and electric insulation, the modules are laminated and subjected to pressure together with a double layer of TPT, that protects the cells from the weather, and EVA that acts

as adhesive between TPT and cells. The *thermal absorber plate* consists of a thin layer that allows high solar radiation absorption; the materials more used are aluminium, copper and steel. The *refrigerant tubes* are usually placed in the photovoltaic modules middle to optimize the thermal exchange. The *insulator*, placed on the collector inferior surface, aims at decreasing the outward thermal dispersions and avoiding the condensate formation; for this reason materials with a low thermal conductivity are used, as foam polyurethane and polystyrene. The whole collector is assembled in a light loom, generally realized in aluminium, and is placed on a steel frame to fix the position according to the chosen tilt angle to tap the higher sun energy. The dimension of each module considered is  $1.3\ m^2$  with a peak power of  $0.18\ kW_p$ , and the photovoltaic cells total area is about  $7.2\ m^2$ . Photovoltaic cells in single-crystal silicon have been considered with an electric efficiency of about 15%. Moreover, the following working conditions have been used in the model: a removable covering glaze with high transmittance, a thermal absorber plate in aluminium with high absorption coefficient, copper tubes with high conductivity, an insulating layer of foam polyurethane, the tubes pitch equal to 150 mm, tilt angle equal to  $30^{\circ}$ , south orientation of the panels and environment data related

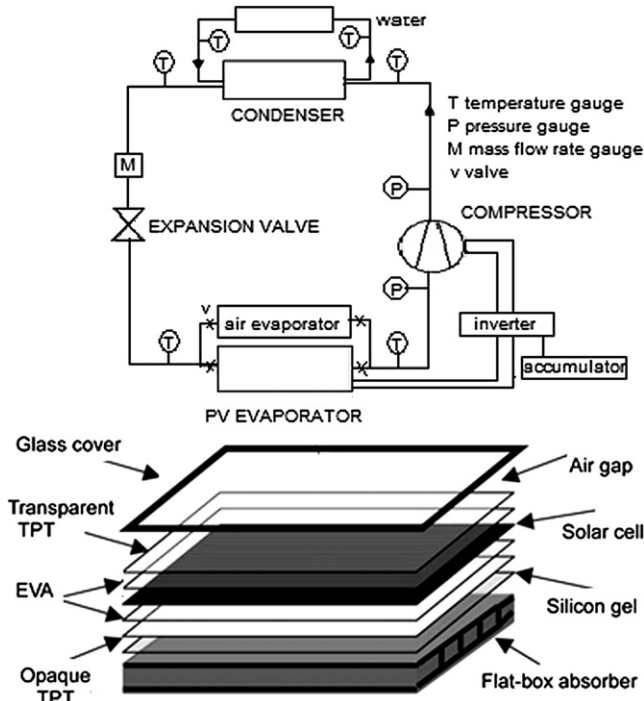


Fig. 1. Heat pump and photovoltaic evaporator scheme.

to Southern Italy. The panels electric terminals are linked to an inverter able to transform the direct current available into alternate current at 220 V, that can be either introduced into the grid, with an outlet electricity meter, or used to supply the compressor or stored in a battery where it could be taken overnight or during cloudy days. Generally, when the water-cooled condenser operates, the circulating water might support space heating and domestic water heating through specific heat exchange devices that in the model have been simulated by a tank that feeds water to the condenser. The water mass flow rate is about 0.2 kg/s; the water temperature is variable in the range 30–55 °C. When the water temperature changes there is a control that fixes the set point required.

### 3. Model of the photovoltaic evaporator and heat pump

#### 3.1. Evaporator

The PV evaporator has been considered as a system that consists of different layers that exchange thermal energy and are identified according to a nodal approach. The energy balance equations for each layer are related to: covering glaze node, photovoltaic modules plate node, thermal absorber plate node, refrigerant tube node, refrigerant node and inferior insulator node (Fig. 1).

##### Covering glaze node

$$m_g c_g \frac{dT_g}{dt} = h_{ag} A_{ag} (T_a - T_g) + \alpha_g \dot{G} - \varepsilon_g \sigma A (T_g^4 - T_s^4) + h_{gp} A_{gp} (T_p - T_g) + \frac{\sigma A_{gp} (T_p^4 - T_g^4)}{\frac{1}{\varepsilon_g} + \frac{1}{\varepsilon_p} - 1} \quad (1)$$

##### Photovoltaic modules plate node

$$m_p c_p \frac{dT_p}{dt} = h_{gp} A_{gp} (T_g - T_p) + \frac{\sigma A_{gp} (T_g^4 - T_p^4)}{\frac{1}{\varepsilon_g} + \frac{1}{\varepsilon_p} - 1} + h_{bp} A_{bp} (T_b - T_p) + (\alpha\tau)_p \dot{G} - \dot{I}_{pv} \quad (2)$$

##### Thermal absorber plate node

$$m_b c_b \frac{dT_b}{dt} = h_{bt} A_{bt} (T_t - T_b) + h_{bp} A_{bp} (T_p - T_b) + h_{bi} A_{bi} (T_i - T_b) \quad (3)$$

##### Refrigerant tube node

$$m_t c_t \frac{dT_t}{dt} = h_{bt} A_{bt} (T_b - T_t) + h_{it} A_{it} (T_i - T_t) + h_{rt} A_{rt} (T_r - T_t) \quad (4)$$

##### Refrigerant node

$$m_t c_t \frac{dT_t}{dt} = -h_{rt} A_{rt} (T_t - T_r) + \dot{Q}_{ev} \quad (5)$$

##### Insulator node

$$m_i c_i \frac{dT_i}{dt} = h_{bi} A_{bi} (T_b - T_i) + h_{ti} A_{ti} (T_t - T_i) + h_{ai} A_{ai} (T_a - T_i) \quad (6)$$

Related to the model equations some terms have been determined:

- $\tau_g = \exp\left[-\Lambda s_g \left(1 - \frac{\sin^2 \theta_1}{R_g^2}\right)^{-0.5}\right]$  is the glaze transmittance (Bouguer law) where the glaze extinction coefficient ( $\Lambda$ ) is equal to 4, the glaze covering thickness ( $s_g$ ) is equal to 4 mm,  $\theta_1 = 45^\circ$  and  $R_g = 1.5-1.8$ .
- $(\alpha\tau)_p = \frac{\tau_{EVA} \alpha_{pv}}{1 - (1 - \alpha_{pv})r}$  is the actual absorption coefficient of the photovoltaic modules plate [15], where  $\tau_{EVA} = \frac{1-r}{1+r}$  is the EVA transmittance coefficient and  $r = \frac{\sin^2(\theta_1 - \theta_2)}{\sin^2(\theta_1 + \theta_2)} + \frac{\tan^2(\theta_1 - \theta_2)}{\tan^2(\theta_1 + \theta_2)}$ .
- $A_{ag} = A_{gp} = A$ , and the areas  $A_{pb}$ ,  $A_{ti}$ ,  $A_{bi}$ ,  $A_{bt}$ ,  $A_{tr}$  of the contact surfaces have been determined in terms of the tube inside and outside diameters ( $D_i = 6$  mm;  $D_o = 8$  mm), the  $A$  value, the photovoltaic collector width, the tube length.

The heat transfer coefficients of the photovoltaic modules, the absorber, the refrigerant tube and the insulator have been determined in terms of the respective thermal conductivities and thicknesses. As for the heat exchange between covering glaze and insulator with outdoor air, the unitary convective conductances have been determined in terms of air velocity [16]. The refrigerant fluid at the evaporator outlet, whose temperature depends on the  $I$  and  $T_o$  values variable with the time, is generally considered in the model in superheated vapour conditions, as it absorbs solar energy and fully evaporates in the PV heat exchanger. The evaporation power depends on the daily variation of the solar radiation intensity, the PV evaporator area and the thermal efficiency [14].

#### 3.2. Condenser

Referring to the condenser, differential equations of the first order have been considered, where the unknowns are the refrigerant and water temperatures at the condenser outlet; the first member presents a store term, the second member the input and output thermal fluxes:

$$m_{tc} c_{tc} \frac{dT_{tc}}{dt} = h_{tc,r} A_{tc,r} (T_r - T_{tc}) - \dot{Q}_{co} \quad (7)$$

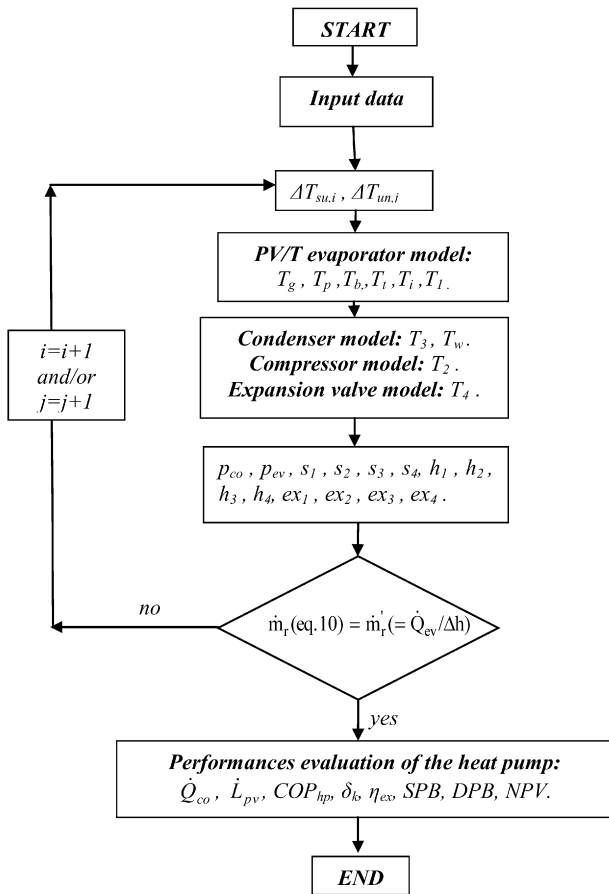


Fig. 2. Model flowchart.

3.3. Compressor and expansion valve

The compressor suction and discharge temperatures are linked by the equation:

$$T_2 = T_1 \left( \frac{P_{co}}{P_{ev}} \right)^\epsilon \tag{9}$$

and the refrigerant mass flow rate is equal to:  $\dot{m}_r = \frac{\eta_r \dot{m} V}{v_1}$ . As for the expansion valve the equation considered is:

$$\dot{m}_r = H_{va} A_{va} \sqrt{2 \rho_{in,va} (p_{co} - p_{ev})} \tag{10}$$

where the evaporation and condensation pressures are obtainable by means of the software Refprop [18] and  $H_{va}$  is the valve characteristic coefficient.

3.4. Thermo-economic analysis

As for the PV heat pump performances, the daily solar radiation allows an energy and costs saving in comparison with a traditional heat pump working under the same conditions. In particular, the compressor and the evaporator are the PV heat pump components principally influenced by the solar radiation. In order to compare the photovoltaic and traditional heat pump performances from the thermo-economic point of view, it is possible to use the following equation [19]:

$$\frac{\partial C_{tot}}{\partial x_k} = c_F \left( \frac{\partial F_{tot}}{\partial x_k} \right) t + \nu \left( \frac{\partial C_k}{\partial x_k} \right) \tag{11}$$

where  $C_{tot}$  (€/year) is the total cost,  $x_k$  is the optimization variable (solar radiation),  $F_{tot}$  (kW) is the external resource, or fuel, consumed by the system (electric power required by the compressor, whose variation corresponds to the compressor destroyed exergy variation [19]),  $c_F$  (€/kWh) is the fuel cost per unit exergy (unit cost of the compressor electric energy),  $t$  (h/year) is the working time,  $\nu$  (1/year) is the amortization coefficient,  $C_k$  (€) is the generic component cost. A finite difference form of the Eq. (11) is:

$$\Delta C_{tot} = c_F \Delta F_{tot} t + \nu \Delta C_k \tag{12}$$

$$m_w c_w \frac{dT_{w,out}}{dt} = \dot{Q}_{co} - \dot{m}_w c_w (T_{w,out} - T_{w,in}) \tag{8}$$

where the condensation power is determined by means of the heat exchanger design equation [17]. The refrigerant fluid at the condenser outlet is generally in subcooled liquid conditions.

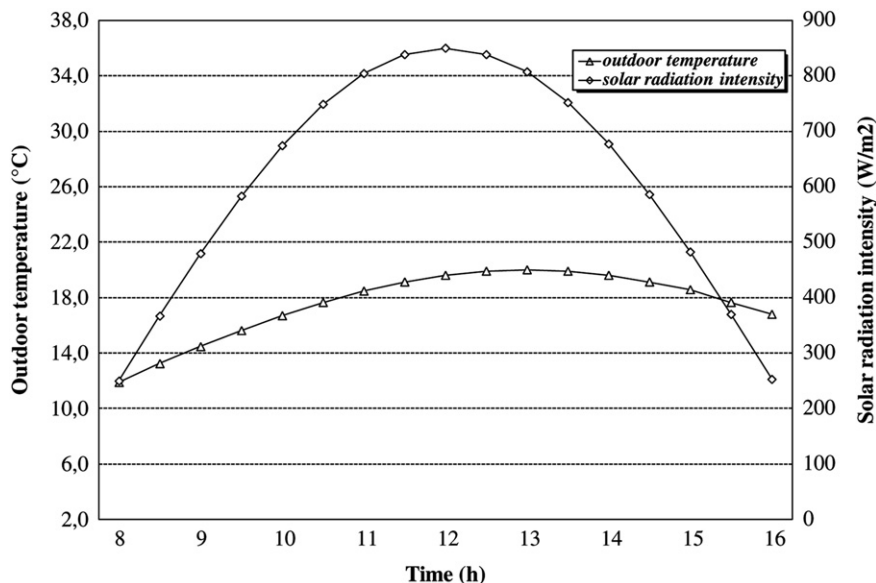


Fig. 3. Solar radiation intensity and outdoor temperature values.

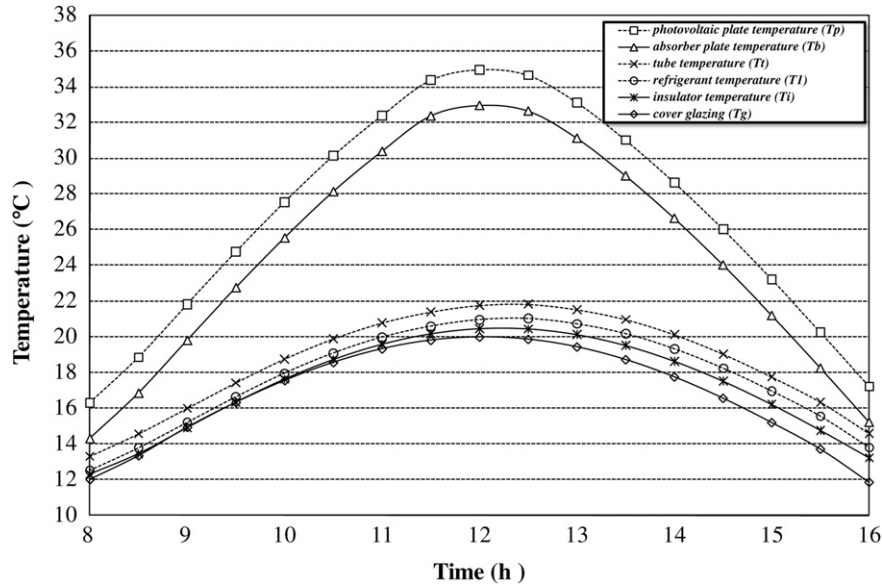


Fig. 4. Photovoltaic evaporator temperatures determined by means of the model.

The Eq. (12) allows to compare from the thermoeconomic point of view the working of the photovoltaic and traditional heat pumps, and then to calculate the economic indexes SPB, DPB and NPV [20]. Moreover, the heat pump COP, the electric, thermal and global efficiency values of the photovoltaic module are equal to:

$$COP_{hp} = \frac{\dot{Q}_{co}}{\dot{L}_{cp}}; \eta_{el} = \frac{\dot{L}_{pv}}{IA_c}; \eta_t = \frac{\dot{Q}_{ev}}{IA_c}; \eta_{tot} = \frac{\dot{Q}_{ev} + \dot{L}_{pv}}{IA_c} \quad (13)$$

where the electrical efficiency depends on the solar cells efficiency and covering factor values, and the PV plate absorption and transmittance coefficients; the photovoltaic power depends on electrical efficiency, solar radiation intensity and collector area [12].

4. Results and discussion

The PV evaporator model consists of six first order linear differential equations whose unknowns are the layers temperatures. The nodal approach and homogeneous properties for each layer, related to density and temperature, are considered without evaluating the spacial distribution. Each equation has as first member the store term, and then the temperature variation with the time, and as second member the thermal and electrical energy fluxes; the photovoltaic energy terms are only present in the covering glaze and solar cells equations. In order to solve the photovoltaic heat pump dynamic model, a program realized with the Matlab software [21] has been used with some simplifying

hypotheses; the model flowchart is reported in Fig. 2. The system input data are the solar radiation intensity and the environment temperature (Fig. 3) that influence the photovoltaic and evaporation powers. These data are related to a typical temperature of the month of November in Southern Italy [22], but other values of  $I$  and  $T_o$  can be considered in the model. The evaporator input data are: collector layers thickness ( $s_i$ ), outside ( $D_o$ ) and inside ( $D_i$ ) diameters of the evaporator tube with its pitch ( $z$ ), tube length ( $L_t$ ) evaluated in terms of the step with the tubes arrangement in the modules prevalent direction, total and effective areas of the PV collector, mass ( $m_i$ ) and specific heat ( $c_i$ ) of the evaporator layers and the condenser tube, tilt and azimuth angles, evaporator components density ( $\rho_i$ ), thermal conductivity ( $k_i$ ) and heat transfer coefficients ( $h_i$ ), air velocity ( $u_a$ ), glaze absorber plate and solar cells emissivity, solar cells efficiency and covering factor ( $\beta_{cf}$ ) values, heat exchangers compressor and expansion valve input data. In the simulation the outdoor temperature has been chosen as initial value of the evaporator nodes temperatures, and the superheating and undercooling values are varied until the refrigerant mass flow rate determined by the Eq.(10) is equal to the value obtained by the evaporator energy balance. The PV evaporator layers temperatures have been determined (Fig. 4) referring to operating hours included among eight in the morning and four in the afternoon, when the gain of electric and thermal energy is possible and larger. In particular, all temperatures follow the parabolic trend of  $I$  and  $T_o$ , and reach the maximum value around noon. In Table 1 the daily variation of the absorber plate temperature according to the

Table 1 Data related to the photovoltaic evaporator.

Outdoor conditions			Photovoltaic evaporator			Adsorber plate temperature		
Hour	$T_o$ (°C)	$I$ (W/m <sup>2</sup> )	$\eta_{el}$	$\eta_t$	$L_{pv}$ (kW)	$T_b$ ( $\beta_{cf} = 0.5$ )	$T_b$ ( $\beta_{cf} = 0.7$ )	$T_b$ ( $\beta_{cf} = 0.9$ )
8	11.9	250	0.138	0.823	0.248	14.7	14.3	13.8
9	14.5	480	0.138	0.654	0.476	20.3	19.7	19.3
10	16.7	674	0.139	0.553	0.674	26.0	25.5	25.1
11	18.5	804	0.140	0.528	0.810	30.8	30.4	29.9
12	19.6	850	0.142	0.520	0.868	33.6	33.0	32.6
13	20.0	807	0.140	0.528	0.813	31.6	31.1	30.7
14	19.6	677	0.139	0.565	0.677	27.1	26.7	26.1
15	18.6	483	0.138	0.653	0.479	21.8	21.3	20.7
16	16.8	253	0.137	0.843	0.249	15.6	15.2	14.7

**Table 2**  
Properties values of the refrigerant fluid in the main cycle points.

Refrigerant fluid properties						
hour	$p_1$ (Mpa)	$p_2$ (MPa)	$T_1$ (°C)	$T_2$ (°C)	$T_3$ (°C)	$T_4$ (°C)
8	0.653	1.29	12.5	51.0	30.2	8.5
9	0.701	1.55	15.2	58.0	36.0	10.9
10	0.758	1.81	18.0	64.3	42.3	13.7
11	0.815	2.00	20.0	68.3	46.3	16.3
12	0.839	2.06	21.0	69.4	47.4	17.2
13	0.833	1.97	20.7	67.8	45.8	16.7
14	0.798	1.75	19.3	62.9	40.9	15.5
15	0.741	1.53	17.0	57.4	35.4	12.8
16	0.674	1.32	13.8	51.7	30.1	9.5

photovoltaic cells covering factor ( $\beta_{cf}$ ) value, has been reported. A higher value of  $\beta_{cf}$  results in more solar energy converted into electricity; hence, the mean absorber plate temperature decreases and the PV module electric efficiency increases because of the more favorable temperature conditions. As for the refrigerant fluid operating in the PV heat pump, the properties values are reported in Table 2. It can be observed that the evaporation pressure varies during the day like the evaporation temperature and the solar radiation intensity, and reaches the maximum value around noon. Besides, the thermal energy absorbed from the PV evaporator allows higher condensation power and temperature values. The compression ratio and refrigerant mass flow rate values vary with time, depending on the evaporation and condensation pressures and the water temperature. Hence, the heat pump COP improves when the solar radiation enhances the condenser capacity and the evaporation temperature and pressure values; in Fig. 5 the values of the compressor input, evaporation and condensation powers and the COP are reported to represent the PV heat pump global performances. It has been useful to validate the system performance by means of experimental data available in literature in order to give greater credibility to the thermoeconomic model described in this paper. In [14] an experimental heat pump, whose evaporator works as PV collector, is presented. In particular, in addition to the operating conditions analyzed in this paper, the model has been also made to run under the same working conditions of the experimental tests realized in [14] in terms of solar radiation intensity, environment temperature, collector characteristics, water temperature and refrigerant fluid; in [14] the water temperature rises to 55 °C. By running the model in the same range

of water temperatures, average values of the condensation power and the COP have been obtained with a percentage deviation of about 6% from the experimental values [14]; the precise comparison also for fixed hours of the day leads to similar percentage deviations.

The main aim is to compare the traditional and PV heat pumps by means of a thermoeconomic analysis; the principal difference between the two systems is represented by the PV evaporator. The PV system is more convenient than the traditional system from the energy point of view, because it can reduce or even eliminate the compressor electrical consumptions both directly and indirectly. In the direct way the compressor is powered by photovoltaic modules independent of the national grid. The solar radiation intensity increase can indirectly improve the compressor and heat pump performances, by increasing both the condenser capacity and the evaporation temperature that determines a decrease of the compression ratio and the compressor electric consumptions from eight in the morning and noon. It results in a reduction of the compressor destroyed exergy and then of the electric power required by the compressor [19]. Referring to a sunny day, in Fig. 6 it is shown that the highest exergy losses occur in the PV evaporator and the compressor, followed by the condenser and expansion valve respectively. The components efficiency defects decrease gradually from early in the morning to noon. In particular, the higher  $I$  and  $T_o$  values and the lower set value of the  $T_w$  are all advantageous for improving the compressor performance. The PV evaporator operating at lower temperatures results in more exergy loss; the higher evaporation temperature is preferable. Hence, the equations (11) and (12) allow to compare from the thermoeconomic point of view and under the same working conditions, the traditional and photovoltaic heat pumps. The main photovoltaic heat pump components not included in a traditional heat pump are PV evaporator, inverter and accumulator that involve higher initial costs, but allow to use electricity throughout the year. The economic results obtained in this paper take into account the costs deduced by the literature because there is not a mass production of the described system yet. In particular, the overall PV system cost is about 400 €/m<sup>2</sup> [23] that takes into account installation and operating costs. The electric power generated by PV panels might be either introduced into the national grid or used to supply the compressor or stored in an accumulator, where it could be taken overnight or during cloudy days. This

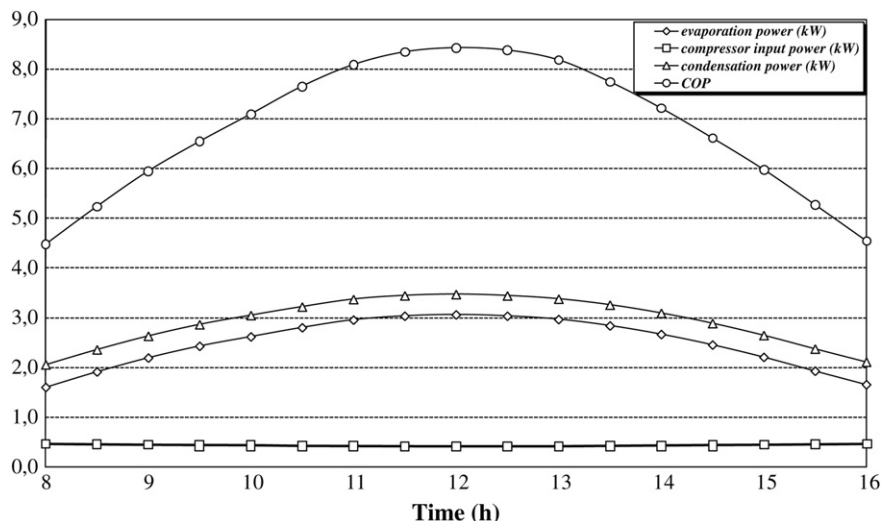


**Fig. 5.** Condensation, compression, evaporation powers and COP.

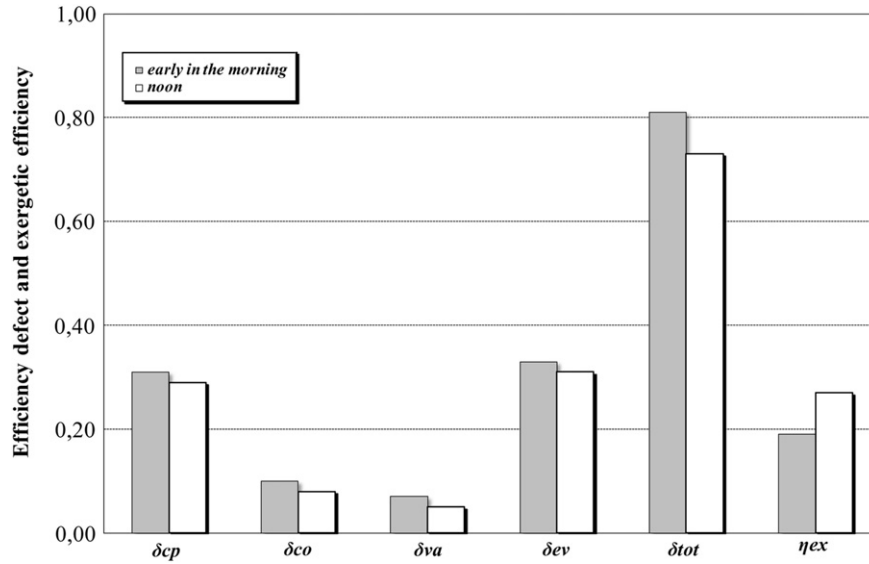


Fig. 6. Efficiency defects and exergetic efficiency.

analysis takes into account the energy incentive proceeds in favour of the photovoltaic systems, provided by [24] and equal to about 0.40 €/kWh<sub>el</sub>. The PV evaporator of 1 kW<sub>p,el</sub>, considered in this paper, allows to obtain both electric annual gain and heat gain. The heat gain during the day is fully used in winter for domestic hot water and in summer if the PV evaporator works instead of the air cooling evaporator. In particular, the heat gain allows during a sunny day, but not at night or when it is cloudy, both an increase of the evaporation and condensation powers and a compressor electrical power decrease. This allows a higher COP and a compressor electric power consumption lower in comparison with a traditional heat pump. Hence, the electricity, that comes from the electric annual gain and the electric power saving obtained from the heat gain, allows both to heat domestic hot water all year and cool in summer without the need of the national grid. In particular, Fig. 5 and Table 1 show respectively the values of the compressor power consumption and the photovoltaic power together with the PV evaporator electric and thermal efficiencies values. In particular, the compressor power varies in the range 0.41–0.46 kW, and the compressor daily

electricity consumption is 3.9 kWh<sub>el</sub>. The PV output power varies in the range 0.25–0.87 kW and the total daily electricity is 5.3 kWh<sub>el,pv</sub>; as every sunny day there is an electricity surplus of about 1.4 kWh<sub>el</sub>, the system is able to operate in a self-sufficient manner. Hence, the PV evaporator of 1 kW<sub>p,el</sub>, considered in this paper, is capable of producing in Southern Italy about 1500 kWh<sub>el</sub>/year [22]. This is, for example, the average electric energy demand of a traditional heat pump to heat the domestic water and to cool in summer, related to a typical Southern Italy house of about 80 m<sup>2</sup> occupied by four people with a demand of about 200 l/day of hot water, whose temperature difference is 30 °C, and 400 h of summer conditioning with a cooling load of about 25 W/m<sup>3</sup> [22]. Hence, a PV evaporator of 1 kW<sub>p,el</sub> allows to meet the demands for domestic hot water and summer cooling, with an air evaporator that works in parallel with the PV evaporator, referring to domestic consumers of Southern Italy where the solar radiation intensity is higher [22]. Finally, in the thermo-economic analysis all the electricity obtained or saved with a PV evaporator of 1 kW<sub>p,el</sub>, both for heating domestic water and for summer cooling, has been considered. Referring to an

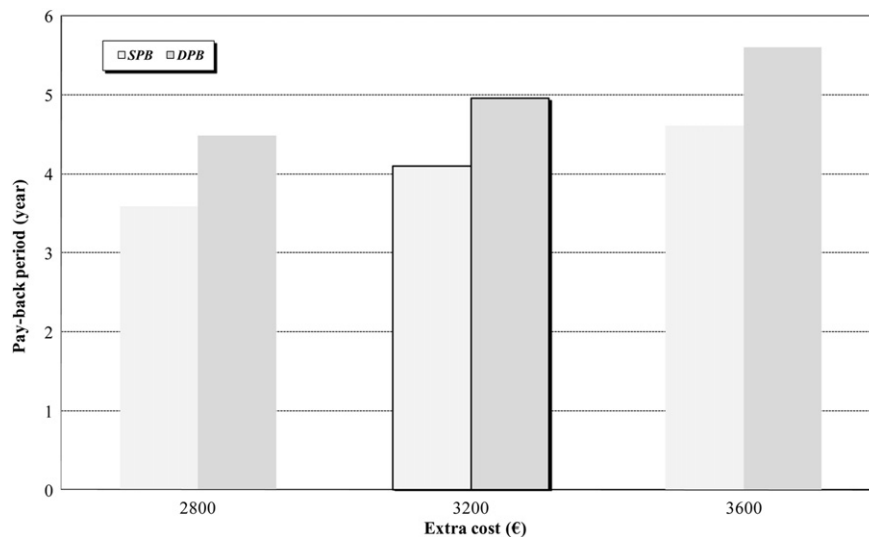


Fig. 7. SPB and DPB values.

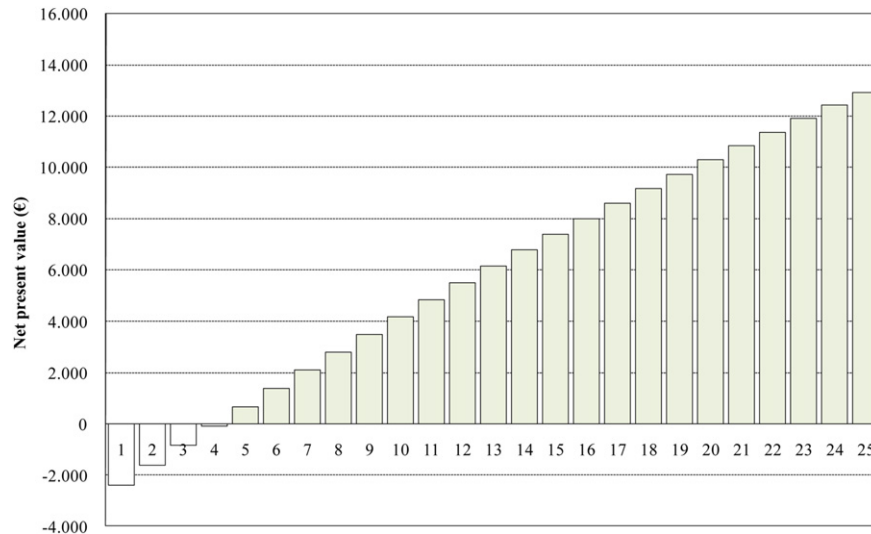


Fig. 8. NPV values.

amortization coefficient of 0.08 1/year, a discounting back rate of 0.05 and twenty five years the plant life, the economic indexes SPB and DPB have been determined (Fig. 7). Under these conditions the cost surplus of the PV heat pump considered in this paper is equal to about 3200 € [23], but the PV modules costs are changing and therefore an economic sensitivity analysis has been realized varying the PV system cost between 2800 € and 3600 € (Fig. 7). In Fig. 8 the NPV values related to a PV system cost of 3200 € are reported. In particular, the NPV is positive after about four years; generally, it depends on the plant location and efficiency.

## 5. Conclusions

Aim of this paper has been the study of a photovoltaic heat pump model from the energy, exergy and economic point of view. The analytical model has been solved by means of a program realized with the Matlab software using some simplifications. The model results have been obtained related to the PV evaporator and heat pump in terms of the evaporator layers temperatures, the refrigerant fluid properties in the main cycle points, the thermal and mechanical powers and the efficiencies that characterize the plant performances. The theoretical results have been also compared with some experimental values available in literature pointing out a low percent deviation. This PV system could also operate where the electric energy is not available. Moreover, this study has allowed to compare the traditional and photovoltaic heat pumps under the same working conditions; the PV heat pump COP is higher respect to a traditional plant. In particular, a thermoeconomic analysis has been carried out in terms of exergy destruction rates and economic indexes. Finally, all electricity obtained or saved with a PV evaporator of 1 kW<sub>p,el</sub> and used both to heat the domestic water and to cool in summer, has allowed to meet the PV evaporator cost with a SPB of about four years.

## References

- [1] D.S. Kim, C.A. Infante Ferreira, Solar refrigeration options a state of the art review. *International Journal of Refrigeration* 31 (2008) 3–15.
- [2] D. Zambrano, C. Bordonsb, W. Garcia-Gabina, E.F. Camachob, Model development and validation of a solar cooling plant. *International Journal of Refrigeration* 31 (2008) 315–327.
- [3] C. Hildbrand, Ph. Dind, M. Pons, F. Buchter, A new solar powered adsorption refrigerator with high performance. *Solar Energy* 77 (2004) 311–318.
- [4] H. Vidal, S. Colle, G. dos Santos Pereira, Modelling and hourly simulation of a solar ejector cooling system. *Applied Thermal Engineering* 26 (2006) 663–672.
- [5] H.M. Henning, *Solar-assisted Air-conditioning Handbook in Buildings: A Handbook for Planners*. Springer-Verlag, Wien, 2004.
- [6] T.A. Kattakayaml, K. Srinivasan, Thermal performance characterization of a photovoltaic driven domestic refrigerator. *International Journal of Refrigeration* 23 (2000) 190–196.
- [7] A. Cherif, A. Dhoub, Dynamic modelling and simulation of a photovoltaic refrigeration plant. *Renewable Energy* 26 (2002) 143–153.
- [8] E.C. Kern Jr, M.C. Russell, Combined photovoltaic and thermal hybrid collector systems, in: *Proceedings of the 13th IEEE PV specialist conference*, Washington DC, 5–8 June 1978, 1153–1157.
- [9] F.B. Gorozabel Chata, S.K. Chaturvedi, Analysis of a direct expansion solar assisted heat pump using different refrigerants. *Energy Conversion and Management* 46 (2005) 2614–2624.
- [10] V. Badescu, First and second law analysis of a solar assisted heat pump based heating system. *Energy Conversion and Management* 43 (2002) 2539–2552.
- [11] Y.H. Kuang, R.Z. Wang, L.Q. Yu, Experimental study on solar assisted heat pump system for heat supply. *Energy Conversion and Management* 44 (2003) 1089–1098.
- [12] H.A. Zondag, D.W. de Vries, W.G.V. van Helden, The thermal and electrical yield of a PV-thermal collector. *Solar Energy* 72 (2002) 113–128.
- [13] A. Tiwari, M.S. Sodha, Performance evaluation of a solar PV/T system: an experimental validation. *Solar Energy* 80 (2006) 751–759.
- [14] G. Pei, J. Ji, H.F. He, K.L. Liu, Performance of a solar assisted heat pump using photovoltaic evaporator, in: *Proceedings of 22nd International Congress of Refrigeration*, (ICR07-E2-1434) Beijing, China, 21–26 August 2007.
- [15] J.A. Duffie, W.A. Beckman, *Solar Engineering of Thermal Processes*. John Wiley & Sons Inc, New York, 1991.
- [16] J.H. Watmuff, W.W.S. Charters, D. Proctor, Solar and wind induced external coefficients for solar collectors. *COMPLES 2* (1977) 56.
- [17] Long Fu, Guoliang Ding, Chunlu Zhang, Dynamic simulation of air-to-water dual-mode heat pump with screw compressor. *Applied Thermal Engineering* 23 (2003) 1629–1645.
- [18] Reference Fluid Thermodynamic and Transport Properties Database (REFPROP): Version 8.0, NIST.
- [19] T.J. Kotas, *The Exergy Method of Thermal Plant Analysis*. Krieger Publ.C, Florida, 1995.
- [20] A. Bejan, G. Tsatsaronis, M. Moran, *Thermal Design and Optimization*. John Wiley, New York, 1996.
- [21] Matlab R2007b, The MathWorks.
- [22] ENEA: The Italian National Agency for New Technologies, Energy and the Environment.
- [23] Volker Quaschnig, Technical and economical system comparison of photovoltaic and concentrating solar thermal power systems depending on annual global irradiation. *Solar Energy* 77 (2004) 171–178.
- [24] Italian Ministerial Decree of the 19-02-07 in favour of the photovoltaic systems.